The Oriented Difference-of-Gaussians Model of Brightness Perception

Mark E. McCourt, [1,2], Barbara Blakeslee [1,2], & Davis Cope [3]

[1] Center for Visual and Cognitive Neuroscience
[2] Department of Psychology
[3] Department of Mathematics
North Dakota State University
Fargo, North Dakota, 58108 USA

ABSTRACT

The Oriented Difference-of-Gaussians (ODOG) model of brightness perception is based on linear spatial filtering by oriented receptive fields followed by contrast/response normalization. The ODOG model can parsimoniously predict the perceived intensity (brightness) of regions in many visual stimuli including White's effect. Unlike competing explanations such as anchoring theory, filling-in, edge-integration, or layer decomposition, spatial filtering by the ODOG model accounts for the gradient structure of induction which, while most striking in grating induction, also occurs within the test fields of classical simultaneous brightness contrast and the White stimulus. Because the ODOG model does not require defined regions of interest it can be applied to arbitrary stimuli, including natural images. We give a detailed description of the ODOG model and illustrate its operation on the Black and White Mondrian stimulus similar to that used by Land & McCann [31] to demonstrate their Retinex model of lightness perception/constancy.

1. INTRODUCTION

The Oriented Difference-of-Gaussians (ODOG) model of Blakeslee & McCourt [6] was developed to gauge the degree to which “early” processes in the visual system, such as spatial filtering and contrast/response normalization, could account for human brightness (perceived intensity) percepts in a set of canonical stimuli including the White effect [4,45,46,47], classical simultaneous brightness contrast (SBC) [25] and grating induction (GI) [5,20,34,36,37,49]. The ODOG model successfully predicts changes in the magnitude of the White effect [9] and GI [11] as a function of inducing grating spatial frequency, and the pattern and magnitude of brightness variations in many other stimuli including the Hermann Grid [8], the Gelb Staircase [16,17], the Wertheimer-Benary Cross [4,7,8], Howe's variations on White's stimulus [15,28], Todorovic's [44] and Williams, McCoy, & Purves’ [48] variations on the SBC stimulus [6,12], the checkerboard induction stimulus of DeValois & DeValois [9,19], the shifted White stimulus [9,46], Adelson's Checker-Shadow [1,12] and Corrugated Mondrian stimuli [1,8], including Todorovic's variation [7,8,44], Adelson's Snake stimulus [2,8,12,42], Hillis & Brainard's Paint/Shadow stimulus [12,27], so-called "remote"

brightness induction stimuli [8,10,32,41], and in the probe discs placed in the photographs of Cartier-Bresson [12,22].

Unlike a variety of competing explanations for human brightness perception which include anchoring theory [22,23], filling-in [24], edge-integration [31,39,40], and layer decomposition [3], the ODOG model accounts for the often overlooked but ubiquitous gradient (viz., non-uniform) structure of induction which while most conspicuous in grating induction [6,13,29,30,34,35], also occurs in the Hermann grid [26,43], the Chevreul staircase [18], Mach Bands [33], and in both classical simultaneous brightness contrast and the White stimulus [6,14]. Since the output of the ODOG model is spatially continuous it can be applied to arbitrary stimuli, including natural images.

The utility of the spatial filtering approach embodied by the ODOG model is its success in accounting for brightness percepts in a wide variety of stimuli, ranging from simple to complex, without the adjustment of any parameter values, and its parsimony, which acts as a scientifically necessary counterweight to high-level theories which rely on vaguely specified mechanisms such as unconscious inference, perceptual transparency, Gestalt grouping, and the like. Below we provide a detailed description of the ODOG model and illustrate its operation on Mondrian stimuli similar to those used by Land & McCann [31] to demonstrate their Retinex model of lightness perception/constancy.

2. THE ODOG MODEL

2.1 ODOG Filters

The ODOG model is graphically illustrated in Figure 1. The model is based on 42 oriented difference-of-gaussians filters (Fig. 1a) which represent cortical receptive fields. There are seven spatial scales spaced at octave-intervals (Fig. 1b), and six orientations spaced at 30^o intervals (Fig. 1d). Input patterns are linearly processed by each filter and the filter outputs are combined using a weighting (Fig. 1c) which approximates the shallow low-frequency falloff of the suprathreshold contrast sensitivity function [21].

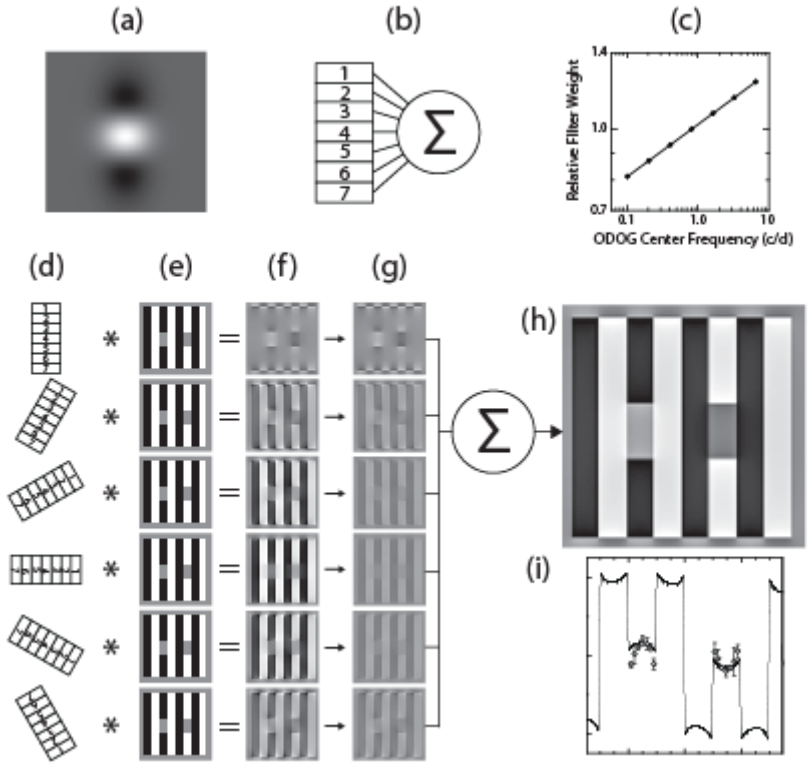

Figure 1: ODOG model applied to White's stimulus. Panel (a) illustrates the spatial structure of an ODOG filter. Panel (b) illustrates that seven filters at octave-interval spatial scales are summed at each filter orientation. Panel (c) shows the center frequencies of the seven ODOG filters and their relative weighting. Panel (d) illustrates the six channel orientations of the ODOG filters summed across scale. Panel (e) shows the White stimulus. Panel (f) shows the result of convolving each stimulus with the multiscale orientation channels shown in (d). Note the relatively higher level of activity for the horizontally oriented channel. Panel (g) shows root mean squared normalized contrast (response) in each orientation channel. Panel (h) shows the summed output across all six contrast-normalized orientation channels. Panel (i) plots a profile of ODOG model output to the White stimulus (black line) and point-by-point brightness matches (open symbols) across the two equiluminant test patches, which demonstrate the gradient nature of induction.

The ODOG filters are described by:

(A.1) $$f_{ODOG}(\sigma_1,\sigma_2,\alpha;x_1,x_2) = \frac{1}{2\pi\sigma_1^2}\exp\left(-\frac{y_1^2+y_2^2}{2\sigma_1^2}\right) - \frac{1}{2\pi\sigma_1\sigma_2}\exp\left(-\frac{1}{2}\left(\frac{y_1^2}{\sigma_2^2}+\frac{y_2^2}{\sigma_1^2}\right)\right)$$
$$= \frac{1}{2\pi\sigma_1}\exp\left(-\frac{y_2^2}{2\sigma_1^2}\right)\left(\frac{1}{\sigma_1}\exp\left(-\frac{y_1^2}{2\sigma_1^2}\right) - \frac{1}{\sigma_2}\exp\left(-\frac{y_1^2}{2\sigma_2^2}\right)\right)$$

where $\sigma_2 > \sigma_1 > 0$ and y_1, y_2 are rotated variables given by:

(A.2) $$y_1 = +\cos(\alpha)\,x_1 + \sin(\alpha)\,x_2 \text{ and } y_2 = -\sin(\alpha)\,x_1 + \cos(\alpha)\,x_2$$

The condition $\sigma_2 > \sigma_1$ ensures that regions of excitation and inhibition are aligned along the y_1-axis. The filters are simple difference of *unit volume* gaussians and are thus balanced (i.e., total filter volume = 0).

The Fourier Transform of ODOG filters is:

(A.3) $F_{ODOG}(\sigma_1, \sigma_2, \alpha; s_1, s_2) = \exp(-2\pi^2\sigma_1^2 t_2^2)\left(\exp(-2\pi^2\sigma_1^2 t_1^2) - \exp(-2\pi^2\sigma_2^2 t_1^2)\right)$

where t_1, t_2 are rotated variables such that:

(A.4) $t_1 = +\cos(\alpha)\, s_1 + \sin(\alpha)\, s_2$ and $t_2 = -\sin(\alpha)\, s_1 + \cos(\alpha)\, s_2$

and six ODOG filters possess orientations at 30° intervals:

(A.5) α = 0°, 30°, 60°, 90°, 120°, 150°

and seven spatial scales arranged at octave intervals:

(A .6) $\sigma_1 = 0.046875°, 0.09375°, 0.1875°, 0.375°, 0.75°, 1.5°, 3.0°$ with $\sigma_2 = 2\sigma_1$

2.2 Input Patterns

Input patterns $p(x_1, x_2)$ are images, shown in Fig. 1(e) as a White stimulus [45]. The two gray bars atop the black and white bars of the background grating are physically identical, yet are dramatically different in brightness. The ODOG model operates on a square patch of space subtending 32° x 32° of visual angle. ODOG filters map input patterns p to output patterns q (which can be negative):

(B.1) $q(\sigma_1, \sigma_2, \alpha; x_1, x_2) = \int_{\mathbb{R}x\mathbb{R}} f_{ODOG}(\sigma_1, \sigma_2, \alpha; y_1 - x_1, y_2 - x_2)\, p(y_1, y_2)\, dy_1\, dy_2$

2.3 Output Patterns

Let $q(\sigma_1, \sigma_2, \alpha, x_1, x_2)$ be the output pattern produced by convolving an ODOG filter with spatial parameters σ_1, σ_2 and orientation α with a given input pattern $p(x_1, x_2)$, as described in (B.1), and shown in Fig. 1(f). The 42 output patterns undergo two additional stages of processing.

First, for each orientation α a weighted summation over filter size is obtained:

(C.1) $Q(\alpha; x_1, x_2) = \int_{all\ \sigma_1} w(\sigma_1)\, q(\sigma_1, 2\sigma_1, \alpha; x_1, x_2)\, d\sigma_1$

where the weight function is $w(\sigma_1) = \left(\frac{8}{3}\sigma_1\right)^{-1/10}$ with σ_1 in degrees. The integral is approximated by the sum:

(C.2) $Q(\alpha; x_1, x_2) \simeq \sum w(\sigma_1)\, q(\sigma_1, 2\sigma_1, \alpha; x_1, x_2)$

where the values of σ_1 are given in (A.6) above.

The root mean square magnitude $\|Q(\alpha; x_1, x_2)\|$ of the output pattern at each orientation α is calculated as:

(C.3) $\|Q(\alpha; x_1, x_2)\|^2 = \int_{\mathbb{R}x\mathbb{R}} \left(Q(\alpha; x_1, x_2)\right)^2 dx_1\, dx_2$

and is used to normalize the magnitude of the neural image [38] across orientation channels (Fig. 1g).

The final output pattern $R(x_1, x_2)$, shown in Fig. 1(h), is obtained by averaging the normalized output patterns over all orientations $(0 \leq \alpha \leq \pi \text{ rad})$:

(C.4) $R(x_1, x_2) = \frac{1}{\pi} \int_{all\ \alpha} \frac{Q(\alpha; x_1, x_2)}{\|Q(\alpha; x_1, x_2)\|}\, d\alpha$

The ODOG model approximates the integral by averaging over the six discrete orientations which are spaced at intervals of 30^o:

(C.5) $R(x_1, x_2) \simeq \frac{1}{6} \sum_{k=0}^{5} \frac{Q(k\pi/6; x_1, x_2)}{\|Q(k\pi/6; x_1, x_2)\|}$

3. THE ODOG MODEL APPLIED TO THE BLACK AND WHITE MONDRIAN STIMULUS OF LAND & McCANN

In introducing the Retinex theory of color constancy Land & McCann [31] described the "Black and White Mondrian" experiment where an array of papers which formed a Mondrian was illuminated by a single light source located at the base of the array. The light provided a vertical gradient of illumination such that a low-reflectance (black) paper at the base of the array (near the light source) was made to reflect the same amount of light as a high-reflectance (white) paper situated at the top of the array (far from the light source). A facsimile of the Land & McCann stimulus is shown in Figure 2(a). Red arrows indicate the upper and lower test patches. Despite being equal in luminance (index value = 128) the lower test patch appears much darker than the upper test patch. Red horizontal lines indicate where profiles of stimulus luminance and ODOG model output are taken. Panels (b) and (c) show profiles of stimulus luminance (black lines) and ODOG model output (red lines), as a function of spatial position. Light gray shading indicates the locations of the test patches. ODOG model output averaged across the upper test patch is 151.9 and is 88.1 for the lower test patch. This exercise demonstrates that the spatial algorithms embodied by ODOG model predict the direction and magnitude of the brightness differences in the "Black and White Mondrian" stimulus (and many others). In this respect the ODOG model is similar to the Retinex model, although a significant difference is that the ODOG model does not incorporate explicit edge integration, thus calling into question the necessity of such a process.

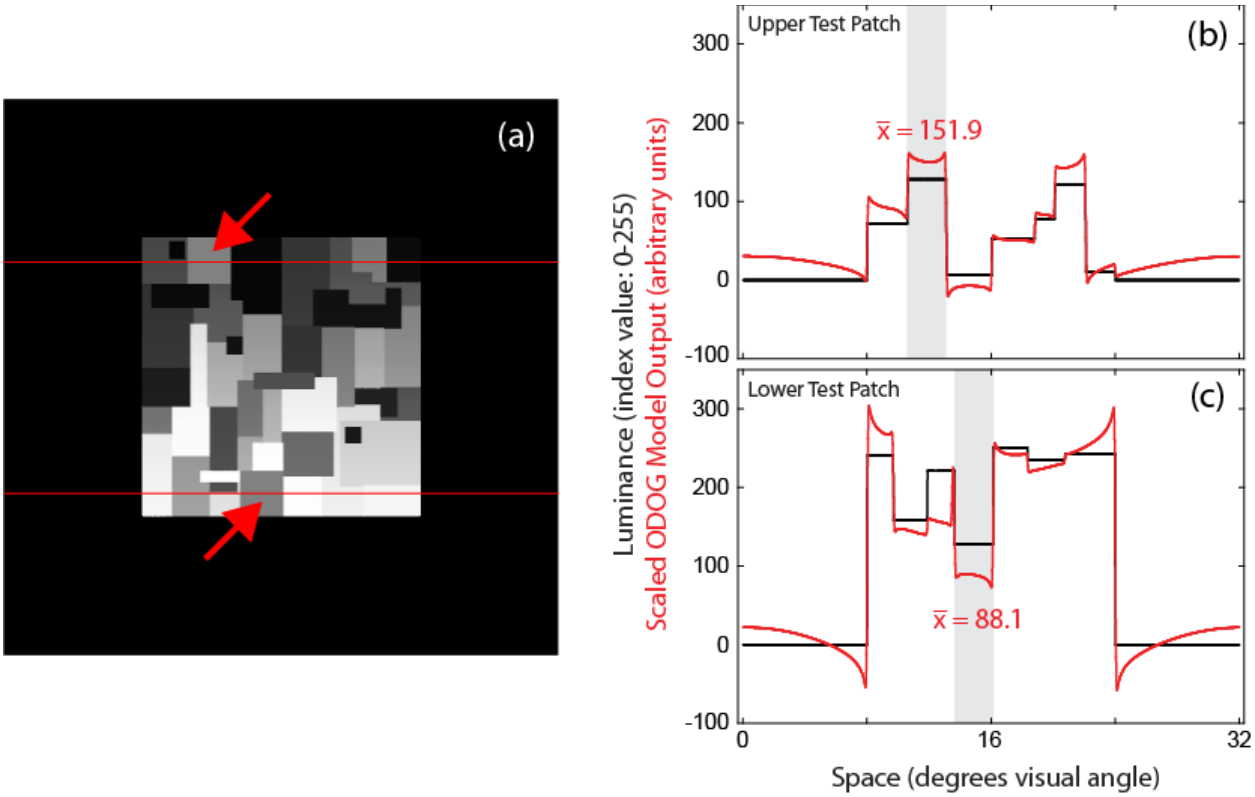

Figure 2: Panel (a) illustrates a facsimile of the original Land & McCann [31] "Black and White Mondrian" stimulus. Red arrows point to the upper and lower test patches. The lower test patch appears darker than the upper test patch, although they are equal in luminance (index value = 128). Red horizontal lines indicate where profiles of stimulus luminance and ODOG model output are taken. Panels (b) and (c) show profiles of stimulus luminance (black lines) and ODOG model output (red lines), as a function of spatial position. Light gray shading indicates the locations of the test patches. ODOG model output averaged across the upper test patch is 151.9 and is 88.1 to the lower test patch. Thus, the ODOG model predicts this brightness illusion and is in this respect similar to the Retinex mode, although there is no explicit stage of edge-integration.

4. ACKNOWLEDGEMENTS

This research was supported by NIH P20 GM103505 (MEM) and NSF BCS 1430503 (BB, MEM). The National Institute of General Medical Sciences (NIGMS) is a component of the National Institutes of Health (NIH). The contents of this report are solely the responsibility of the authors and do not necessarily reflect the official views of the NIH, NIGMS, or NSF. The authors declare no conflict of interest.

5. REFERENCES

1. Adelson, E. H. (1993). Perceptual organization and the judgment of brightness. *Science, 262*, 2042-2044.
2. Adelson, E. H. (2000). Lightness perception and lightness illusions. In Gazzaniga, M. (Ed.): *The New Cognitive Neurosciences* (2nd ed., pp. 339-351). Cambridge, MA: MIT Press.

3. Anderson, B. L. (1997). A theory of illusory lightness and transparency in monocular and binocular images: The role of contour junctions. *Perception, 26*, 419-453.
4. Benary, W. (1924). Beobachtungen zu einem experiment uber helligkeitskontrast. *Psychologische Forschung, 5*, 131-142.
5. Blakeslee, B., & McCourt, M. E. (1997). Similar mechanisms underlie simultaneous brightness contrast and grating induction. *Vision Research, 37*, 2849-2869.
6. Blakeslee, B., & McCourt, M. E. (1999). A multiscale spatial filtering account of the White effect, simultaneous brightness contrast, and grating induction. *Vision Research, 39*, 4361-4377.
7. Blakeslee, B., & McCourt, M. E. (2001). A multiscale spatial filtering account of the Wertheimer-Benary effect and the corrugated Mondrian. *Vision Research, 41*, 2487-2502.
8. Blakeslee, B., & McCourt, M. E. (2003). A multiscale spatial filtering account of brightness phenomena. In Harris, L. & Jenkin, M. (Eds.): *Levels of Perception.* New York, NY: Springer.
9. Blakeslee, B., & McCourt, M. E. (2004). A unified theory of brightness contrast and assimilation incorporating oriented multiscale spatial filtering and contrast normalization. *Vision Research, 44*, 2483-2503.
10. Blakeslee, B., & McCourt, M. E. (2005). A multiscale spatial filtering account of grating induction and remote brightness induction effects: Reply to Logvinenko. *Perception, 34*, 793-802.
11. Blakeslee, B., & McCourt, M. E. (2011). Spatiotemporal analysis of brightness induction. *Vision Research, 51*, 1872-1879.
12. Blakeslee, B., & McCourt, M. E. (2012). When is spatial filtering enough? Investigations of lightness and brightness perception in stimuli containing a visible illumination component. *Vision Research, 60,* 40-50.
13. Blakeslee, B., & McCourt, M. E. (2013). Brightness induction magnitude declines with increasing distance from the inducing field edge. *Vision Research, 78*, 39-45.
14. Blakeslee, B., & McCourt, M. E. (2016). The White effect. In Shapiro, A. & Todorovic, D. (Eds.): *Oxford Compendium of Visual Illusions*. Oxford, UK: Oxford University Press (in press).
15. Blakeslee, B., Pasieka, W., & McCourt, M. E. (2005). Oriented multiscale spatial filtering and contrast normalization: A parsimonious model of brightness induction in a continuum of stimuli including White, Howe and simultaneous brightness contrast. *Vision Research, 45*, 607-615.
16. Blakeslee, B., Reetz, D., & McCourt, M. E. (2009). Spatial filtering versus anchoring accounts of brightness/lightness perception in staircase and simultaneous brightness/lightness contrast stimuli. *Journal of Vision, 9(3): 22*, 1-17, http://journalofvision.org/9/3/22/, doi: 10.1167/9.3.22.
17. Cataliotti, J., & Gilchrist, A. (1995). Local and global processes in surface lightness perception. *Perception & Psychophysics, 57*, 125-135.
18. Chevreul, M. E. (1890). In Martel, C. (Translator): *The Principles of Harmony and Contrast of Colours*. London, UK: Bell.
19. DeValois, R. L., & DeValois, K. K. (1988). *Spatial Vision*. New York, NY: Oxford University Press.

20. Foley, J. M., & McCourt, M. E. (1985). Visual grating induction. *Journal of the Optical Society of America, A2*, 1220-1230.
21. Georgeson, M. A., & Sullivan, G. D. (1975). Contrast constancy: Deblurring in human vision by spatial frequency channels. *Journal of Physiology (London), 252*, 627-656.
22. Gilchrist, A. L. (2006). *Seeing Black and White*. New York, NY: Oxford University Press.
23. Gilchrist, A., Kossyfidis, C., Bonato, F., Agostini, T., Cataliotti, J., Li, X., Spehar, B., Annan, V., & Economou, E. (1999). An anchoring theory of lightness perception. *Psychological Review, 106*, 795-834.
24. Grossberg, S., & Todorovic, D. (1988). Neural dynamics of 1-D and 2-D brightness perception: A unified model of classical and recent phenomena. *Perception and Psychophysics, 43*, 241-277.
25. Heinemann, E. G. (1972). Simultaneous brightness induction. In Jameson, D. & Hurvich, L. M. (Eds.): *Handbook of Sensory Physiology, VII-4 Visual Psychophysics*. Berlin: Springer-Verlag.
26. Hermann, L. (1870). Eine erscheinung des simultanen contrastes. *Pflugers Archiv fur die gesamte Physiologie, 3*, 13-15.
27. Hillis, J. M., & Brainard, D. H. (2007). Distinct mechanisms mediate visual detection and identification. *Current Biology, 17*, 1714-1719.
28. Howe, P. D. L. (2001). A comment on the Anderson (1997), the Todorovic (1997), and the Ross and Pessoa (2000) explanations of White s effect. *Perception, 30*, 1023-1026.
29. Kingdom, F. A. A. (1999). Old wine in new bottles? Some thoughts on Logvinenko's "Lightness induction revisited". *Perception, 28*, 929-934.
30. Kingdom, F. A. A. (2011). Lightness, brightness and transparency: A quarter century of new ideas, captivating demonstrations and unrelenting controversy. *Vision Research, 51*, 652-673.
31. Land, E. H., & McCann, J. J. (1971). Lightness and retinex theory. *Journal of the Optical Society of America, 61*, 1-11.
32. Logvinenko, A. D. (2003). Does the bandpass linear filter response predict gradient lightness induction? A reply to Fred Kingdom. *Perception, 32*, 621-626.
33. Mach, E. (1865). On the effect of the spatial distribution of the light stimulus on the retina. In Ratliff, F. (Ed.): *Mach Bands: Quantitative Studies on Neural Networks in the Retina* (1965), (pp. 253-271). San Francisco, CA: Holden-Day,
34. McCourt, M. E. (1982). A spatial frequency dependent grating-induction effect. *Vision Research, 22*, 119-134.
35. McCourt, M. E., & Blakeslee, B. (1994). A contrast matching analysis of grating induction and suprathreshold contrast perception. *Journal of the Optical Society of America, A, 11*, 14-24.
36. McCourt, M. E., & Blakeslee, B. (2016). Grating induction. In Shapiro, A. & Todorovic, D. (Eds.): *Oxford Compendium of Visual Illusions.* Oxford, UK: Oxford University Press (in press).
37. McCourt, M. E., & Foley, J. M. (1985). Spatial frequency interference on grating induction. *Vision Research, 25*, 1507-1518.

38. Robson, J. G. (1980). Neural images. The physiological basis of spatial vision. In *Visual Coding and Adaptability*, (pp. 177-214). Hillsdale, NJ: Lawrence Erlbaum Associates.
39. Rudd, M. E., & Zemach, I. K. (2004). Quantitative properties of achromatic color induction: An edge integration analysis. *Vision Research, 44*, 971-981.
40. Rudd, M. E., & Zemach, I. K. (2007). Contrast polarity and edge integration in achromatic color perception. *Journal of the Optical Society of America, A, 24*, 2134-2156.
41. Shapley, R., & Reid, R. C. (1985). Contrast and assimilation in the perception of brightness. *Proceedings of the National Academy of Science USA, 82*, 5983-5986.
42. Somers, D. C., & Adelson, E. H. (1997). Junctions, transparency, and brightness. *Investigative Ophthalmology and Visual Science, 38 (Suppl.)*, S453.
43. Spillmann, L. (1994). The Hermann grid illusion: A tool for studying human perceptive field organization. *Perception, 23*, 691-708.
44. Todorovic, D. (1997). Lightness and junctions. *Perception, 26*, 379-395.
45. White, M. (1979). A new effect of pattern on perceived lightness. *Perception, 8*, 413-416.
46. White, M. (1981). The effect of the nature of the surround on the perceived lightness of grey bars within square-wave test gratings. *Perception, 10*, 215-230.
47. White, M., & White, T. (1985). Counterphase lightness induction. *Vision Research, 25*, 1331-1335.
48. Williams, S. M., McCoy, A. N., & Purves, D. (1998). The influence of depicted illumination on perceived brightness. *Proceedings of the National Academy of Sciences, 95*, 13296-13300.
49. Zaidi, Q. (1989). Local and distal factors in visual grating induction. *Vision Research, 29*, 691-697.